

This article was downloaded by:[Bochkarev, N.]
On: 14 December 2007
Access Details: [subscription number 746126554]
Publisher: Taylor & Francis
Informa Ltd Registered in England and Wales Registered Number: 1072954
Registered office: Mortimer House, 37-41 Mortimer Street, London W1T 3JH, UK



Astronomical & Astrophysical Transactions

The Journal of the Eurasian Astronomical Society

Publication details, including instructions for authors and subscription information:
<http://www.informaworld.com/smpp/title~content=t713453505>

Escaping and trapped orbits in a "bare" Seyfert 1 nucleus dynamical model

N. J. Papadopoulos^a; N. D. Caranicolas^a

^a Department of Physics, Section of Astrophysics, Astronomy and Mechanics, University of Thessaloniki, Thessaloniki, Greece

Online Publication Date: 01 August 2007

To cite this Article: Papadopoulos, N. J. and Caranicolas, N. D. (2007) 'Escaping and trapped orbits in a "bare" Seyfert 1 nucleus dynamical model', *Astronomical & Astrophysical Transactions*, 26:4, 301 - 309

To link to this article: DOI: 10.1080/10556790701524442

URL: <http://dx.doi.org/10.1080/10556790701524442>

PLEASE SCROLL DOWN FOR ARTICLE

Full terms and conditions of use: <http://www.informaworld.com/terms-and-conditions-of-access.pdf>

This article maybe used for research, teaching and private study purposes. Any substantial or systematic reproduction, re-distribution, re-selling, loan or sub-licensing, systematic supply or distribution in any form to anyone is expressly forbidden.

The publisher does not give any warranty express or implied or make any representation that the contents will be complete or accurate or up to date. The accuracy of any instructions, formulae and drug doses should be independently verified with primary sources. The publisher shall not be liable for any loss, actions, claims, proceedings, demand or costs or damages whatsoever or howsoever caused arising directly or indirectly in connection with or arising out of the use of this material.

Escaping and trapped orbits in a “bare” Seyfert 1 nucleus dynamical model

N. J. PAPADOPOULOS and N. D. CARANICOLAS*

Department of Physics, Section of Astrophysics, Astronomy and Mechanics,
University of Thessaloniki, 541 24 Thessaloniki, Greece

(Received 26 February 2007)

The nature and behaviour of the orbits in a “bare” Seyfert 1 dynamical model is studied. This model is subject to external perturbation caused by nearby galaxies. Numerical calculations suggest that, when the external perturbation is high the majority of orbits change from regular to chaotic. For higher external perturbations the zero velocity curves open and a number of orbits goes to infinity. In addition to those orbits, there are orbits that do not escape at all. Theoretical evidence shows that these orbits have an additional quasi-integral of motion which is a generalization of the angular momentum of the test particle.

Keywords: Orbits; Seyfert nucleus; Galactic models

1. Introduction

Most astronomers believe that the origin of nuclear activity in galaxies and quasars is still a puzzle. The standard model involves accretion of matter into a compact central object [1]. On the other hand, a detailed understanding of the physical processes leading to nuclear activity in galaxies and quasar activity is still lacking. Furthermore, there is evidence that active galaxies and quasars frequently have close companions. Some show unambiguous signs of tidal interaction such as asymmetries, tails and bridges [2, 3].

During recent years, new kinematic models of Seyfert galaxies have been developed. Most of these models are based on recent, high-resolution long-slit spectra of the narrow-line regions (NLRs) of Seyfert galaxies, obtained with the Space Telescope Imaging Spectrograph (STIS) aboard the Hubble Space Telescope (HST) [4–10].

In the present paper we investigate the structure of orbits in a “bare” Seyfert 1 dynamical model. More correctly we study the motion in a dynamical model composed of a “bare” Seyfert 1 nucleus subject to external perturbations caused by nearby galaxies. The present model does not involve any accretion of matter into a compact central object as was done in other models for active galaxies [11, 12].

*Corresponding author. Email: caranic@astro.auth.gr

There are several reasons for doing this paper: (i) Observations show that Arakelian 120 is a bright Seyfert 1 galaxy with an emission spectrum indicating a “bare” Seyfert 1 nucleus [13]. (ii) Such dynamical studies are rare, therefore the results will be of interest and (iii) it would be nice to compare the present results with those previously obtained for active galaxies and quasars [12, 14].

Our dynamical model is represented by the potential

$$V(x, y) = -\frac{M_n}{(x^2 + y^2 + c_n^2)^{1/2}} - \epsilon xy^2. \quad (1)$$

Here M_n and c_n is the mass and the scale length of the nucleus while ϵ is the strength of the external perturbation. We use a system of galactic units, where the unit of length is 1 kpc, the unit of time is 0.97746×10^8 yr and the unit of mass is $2.325 \times 10^7 M_\odot$. The velocity and energy unit (per unit mass) is 10 km/s and $100 (\text{km/s})^2$, respectively, while G is equal to unity. In the above units we use the values $M_d = 400$, $c_n = 0.25$ kpc, while ϵ is treated as a parameter.

We assume a clockwise rotation with an angular velocity Ω . The corresponding Hamiltonian, which is known as the Jacobi integral, is

$$\begin{aligned} H_J &= \frac{1}{2}(p_x^2 + p_y^2) + V(x, y) - \frac{1}{2}\Omega^2(x^2 + y^2) \\ &= \frac{1}{2}(p_x^2 + p_y^2) + V_{\text{eff}}(x, y) = E_J, \end{aligned} \quad (2)$$

where p_x, p_y are the momenta, per unit mass, conjugate to x and y

$$V_{\text{eff}}(x, y) = V(x, y) - \frac{1}{2}\Omega^2(x^2 + y^2), \quad (3)$$

is the effective potential and E_J is the numerical value of the Jacobi integral.

This article has the following targets: (i) to study the regular and chaotic nature of motion and to connect the transition from regularity to chaos with the values of the parameters entering the potential (3). (ii) To find the escaping orbits as well as the trapped orbits when the zero velocity curves are open. (iii) To present some theoretical evidence in order to support the numerical results.

The layout of the paper is as follows: in section 2 we study the regular and chaotic nature of motion. Section 3 is devoted to the study of escaping and trapped orbits. In the same section some theoretical arguments, are presented, which are used to explain the numerical outcomes. We close with a discussion which is presented in section 4.

2. The nature of motion

As we are interested to obtain a global picture for the nature of motion we shall use the $x - p_x, y = 0, p_y > 0$ Poincare phase plane. The results come from the numerical integration of the equations of motion

$$\ddot{x} = -2\Omega\dot{y} - \frac{\partial V_{\text{eff}}}{\partial x}, \quad \ddot{y} = 2\Omega\dot{x} - \frac{\partial V_{\text{eff}}}{\partial y}, \quad (4)$$

where the dot indicates derivative with respect to the time.

Figure 1 shows the $x - p_x, y = 0, p_y > 0$ Poincare phase plane for the Hamiltonian (2) when $E_J = -160, M_n = 400, c_n = 0.25, \Omega = 1.25$ and $\epsilon = 0.2$. Most of the phase plane is covered by orbits producing invariant curves. This means that the largest part of orbits are regular orbits. The invariant curves surrounding the fixed points (on the left-hand side) corresponding to the direct and the retrograde (on the right-hand side) periodic orbits are produced by the two main families of orbits in the potential (1). As one can see the first invariant point is stable while the second is unstable. In addition to those 1:1 resonant periodic orbits there are also regular orbits producing sets of small islands. These orbits are product of secondary resonances. A small chaotic layer is also seen on the left hand side part of figure 1.

Figure 2 is the same as figure 1 when $\epsilon = 2.2$. Here the two main families of regular orbits continue to exist but they cover only a small area around each of the two periodic points. The rest of the phase plane is covered by a chaotic sea. Therefore, our numerical outcomes suggest that the result of a strong external perturbation is to destroy a large part of regular orbits and to produce an extended chaotic sea.

Comparing figures 1 and 2 we find that the regular area around the invariant point corresponding to the direct periodic orbit is considerably smaller than that around the invariant point corresponding to the retrograde periodic orbit. This can be explained by considering the angular momentum of the two orbits starting near the each of the two invariant points in figure 2. We know that the angular momentum in the rotating potential (3) [15] is given by the expression

$$L = x\dot{y} - \dot{x}y - \Omega(x^2 + y^2). \quad (5)$$

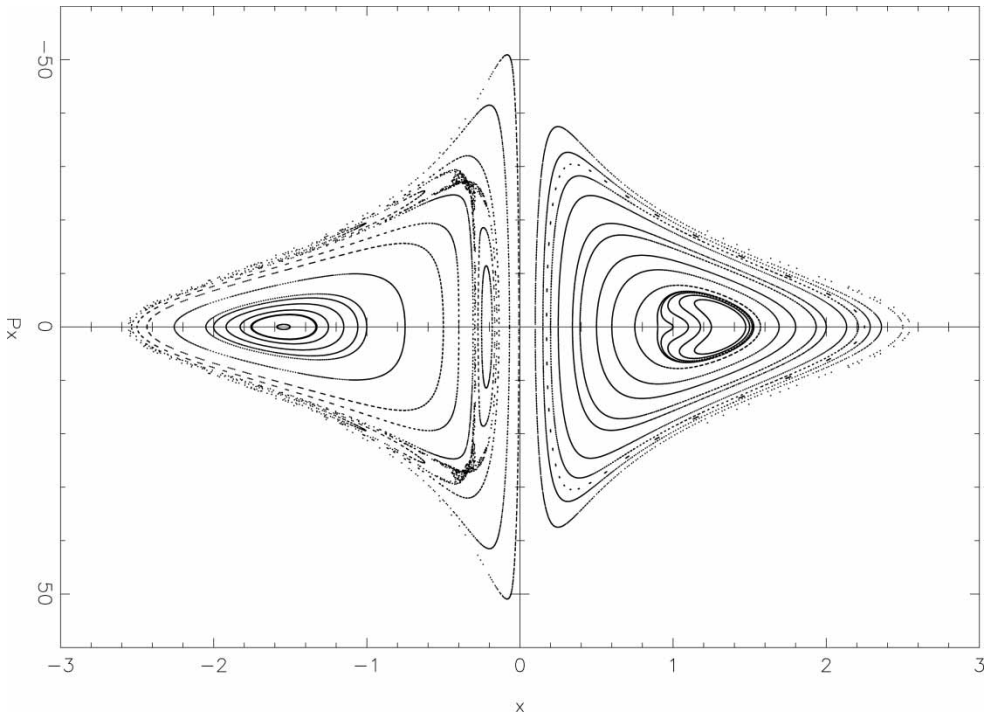


Figure 1. The $x - p_x, y = 0$ phase plane for the Hamiltonian (2) when $E_J = -160, M_n = 400, c_n = 0.25, \Omega = 1.25$ and $\epsilon = 0.2$.

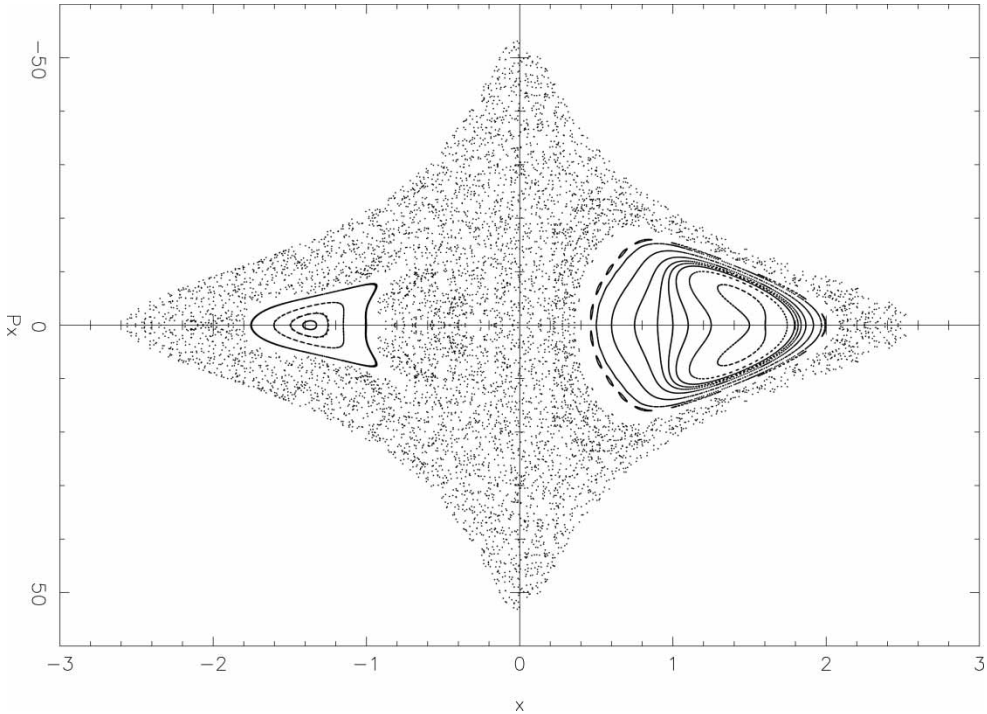


Figure 2. Same as figure 1 when $\epsilon = 2.2$. Note the large chaotic sea.

As L is not conserved we can take its mean value for a time period using the formula

$$\langle L \rangle = \sum_{k=1}^n L_k. \quad (6)$$

For the first orbit, starting near direct invariant point, we take $x = -1.5$, $y = p_x = 0$ while in all cases the value of p_x is found using Jacobi integral. All other parameters are as in figure 2. For this orbit shown in figure 3 we find from (6) $\langle L \rangle = -23.66$. For the second orbit, starting near retrograde invariant point (see figure 4), the initial conditions are $x = 1.5$, $y = p_x = 0$. We find from (6) $\langle L \rangle = 17.94$. The numerical integration was carried for 50 time units while n was taken equal to 5000. We see that direct orbits have negative values of mean angular momentum while retrograde orbits have positive mean values of angular momentum. Therefore the result shown in figure 2 is evident as orbits of small angular momentum become easily chaotic under large perturbations.

3. Escaping and trapped orbits. Theoretical arguments

In this section we study the behaviour of orbits for large external perturbations. In this case the zero velocity curves (ZVCs)

$$V_{\text{eff}}(x, y) = E_J, \quad (7)$$

are open curves and there are cases where the test particle goes to infinity. A large number of orbits (about 500) were calculated in the case when $\epsilon = 2.23$, while all other parameters were taken as in figure 1. The corresponding ZVC is open. Note that the value of ϵ cannot

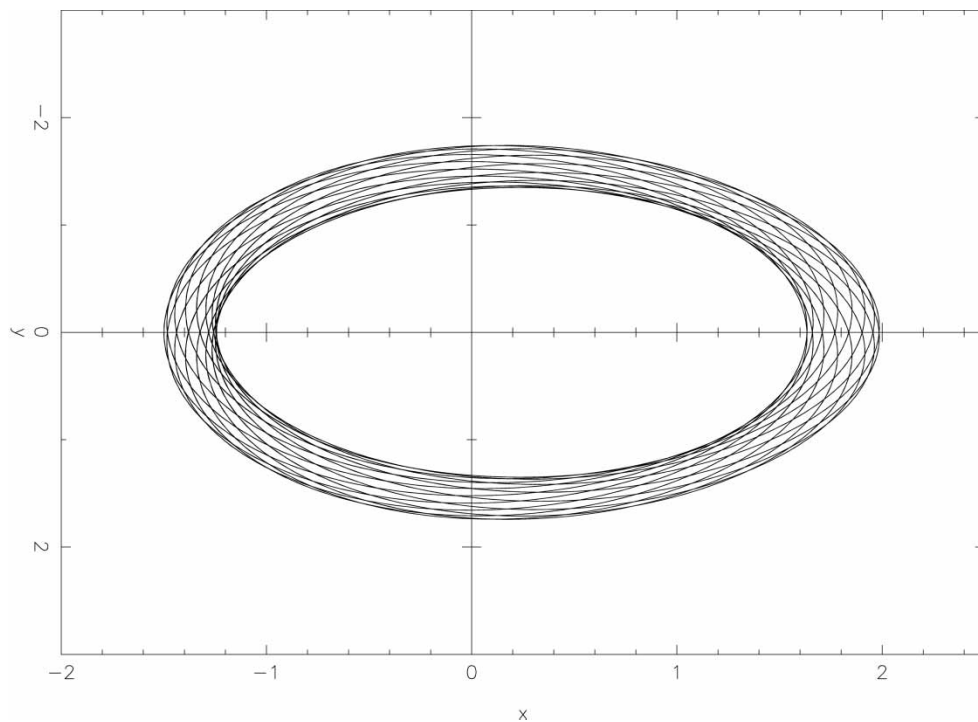


Figure 3. An orbit starting near the direct invariant point. This orbit has a small value of $\langle L \rangle$.

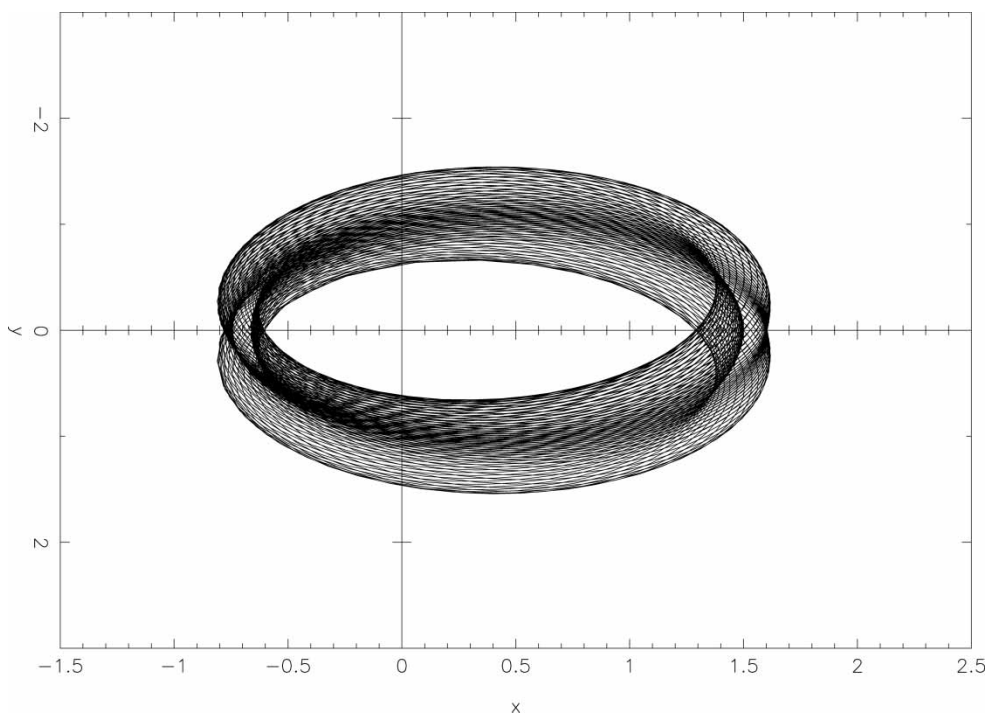


Figure 4. An orbit starting near the retrograde invariant point. This orbit has a large value of $\langle L \rangle$.

be found analytically as in other cases [16]. Numerical calculations suggest that the majority of orbits escape for a time period $T_{\text{esc}} \leq 300$ time units, while there are some cases when the test particle stays inside the ZVC for a time period $T > 2000$ time units. This time period is larger than the age of the universe.

Here we must note that the escape time period T_{esc} depends strongly on the numerical integration program. We must emphasise that when computing the $x - p_x$ phase plane many iterations are used in order to find the $y = 0$ plane. In this case the numerical integration gives small values of T_{esc} . On the other hand, for orbit calculations when a simple integration program is used we find larger escape time periods T_{esc} . All the above mentioned T_{esc} were calculated by the second simple program.

Figure 5 shows the $x - p_x$ phase plane when $\epsilon = 2.23$. As one can see there are orbits that do not escape at all. These trapped orbits are quasi-periodic orbits giving invariant curves on the $x - p_x$ plane surrounding the direct and retrograde periodic points. The outermost curve is the limiting curve

$$\frac{1}{2} p_x^2 + V_{\text{eff}}(x) = E_J. \quad (8)$$

Note that the limiting curve is always closed for all values of ϵ . Therefore, it is evident that, the test particle escapes through the open channels of the ZVC in the configuration $[x - y]$ plane. An escaping orbit is shown in figure 6. Initial conditions $x = -0.5$, $y = p_x = 0$. All other parameters are as in figure 1, while $\epsilon = 2.23$. The orbit escapes after $T = 240$ time units. Here the orbit was plotted for the last 40 time units.

All the numerical calculations were made by the sharp Bulirsh–Stoer method in double precision. The accuracy of the calculations was checked by the constancy of the Jacobi integral which was conserved up to the twelfth significant figure.

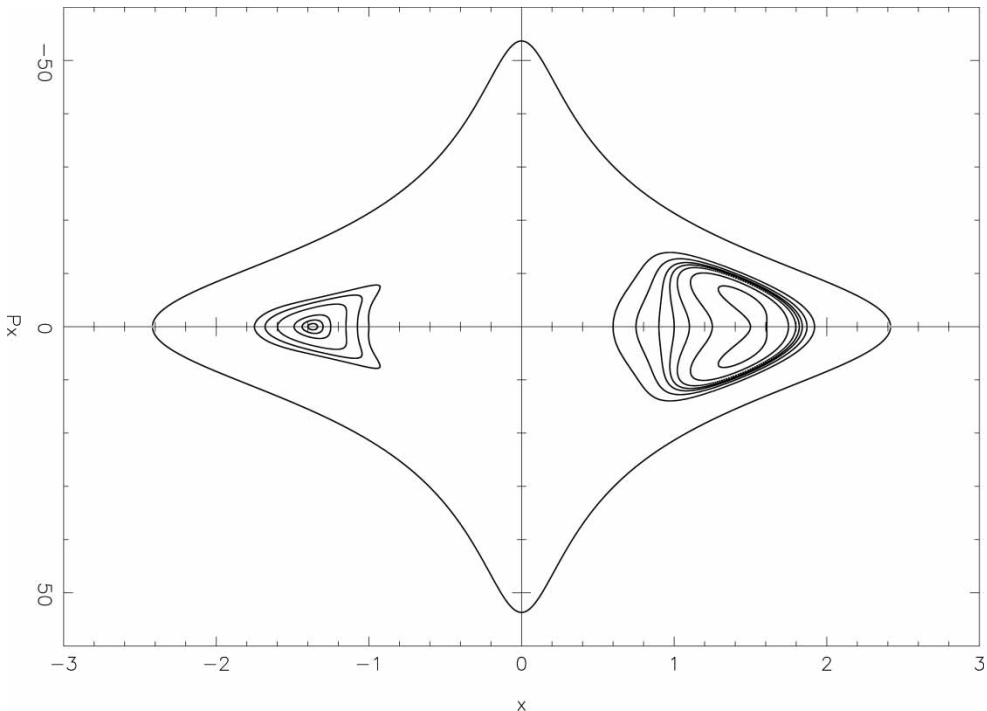


Figure 5. The $x - p_x$ phase plane when $\epsilon = 2.23$. All the invariants curves belong to trapped orbits.

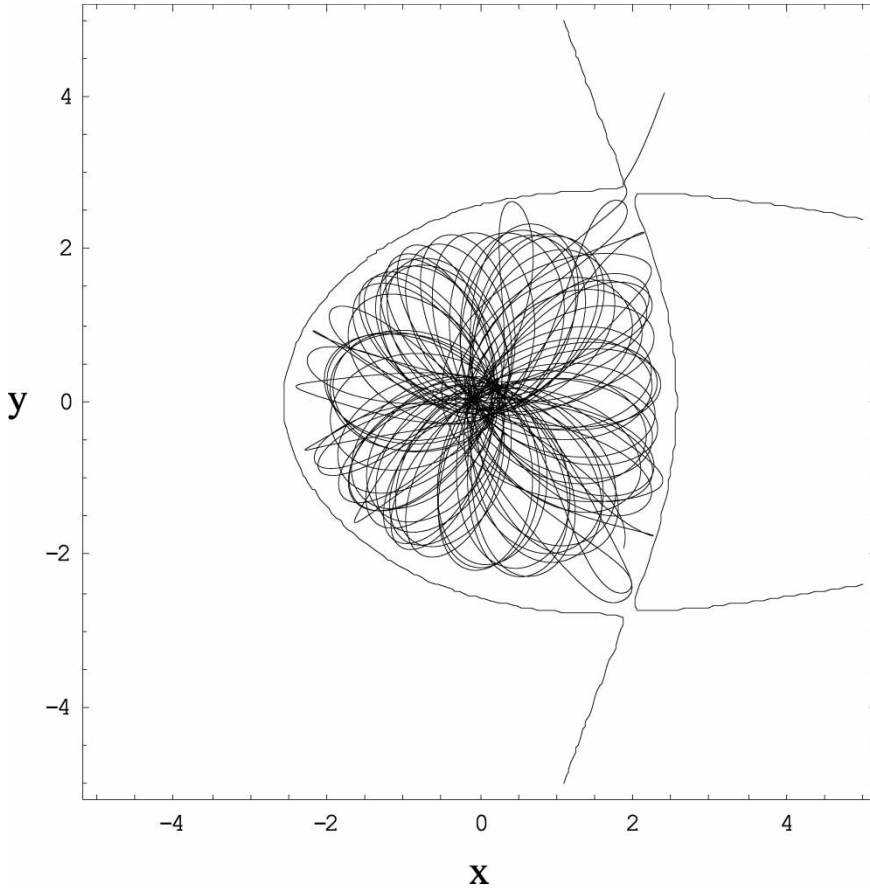


Figure 6. An escaping orbit when $\epsilon = 2.23$. See text for details.

The general characteristics of the system, for small values of ϵ , can be reproduced qualitatively using a quasi-integral of motion [17]. As such a quasi-integral we may consider a generalization of the angular momentum of the test particle, that is

$$\phi = L^2 + 2\Omega x^3 p_y - 2\Omega^2 x^4 - \Omega x^2 - \epsilon x^2. \quad (9)$$

Eliminating p_y between (9) and the energy integral (2) after setting $y = 0$ we obtain

$$\phi(x, p_x) = \left[2E_J + \frac{2M_n}{(x^2 + C_n^2)^{1/2}} + \Omega^2 x^2 - p_x^2 \right] x^2 - \Omega x^2 - \epsilon x^2. \quad (10)$$

Figure 7 shows the curves $\phi(x, p_x) = c$, when $c = 10, 50, 130, 300, 450$ from outside inwards. The values of the parameters are as in figure 1. One can see that the general characteristic of the system is well described by the quantity ϕ . Note that as the value of c increases we get invariant curves closer to the two invariant points.

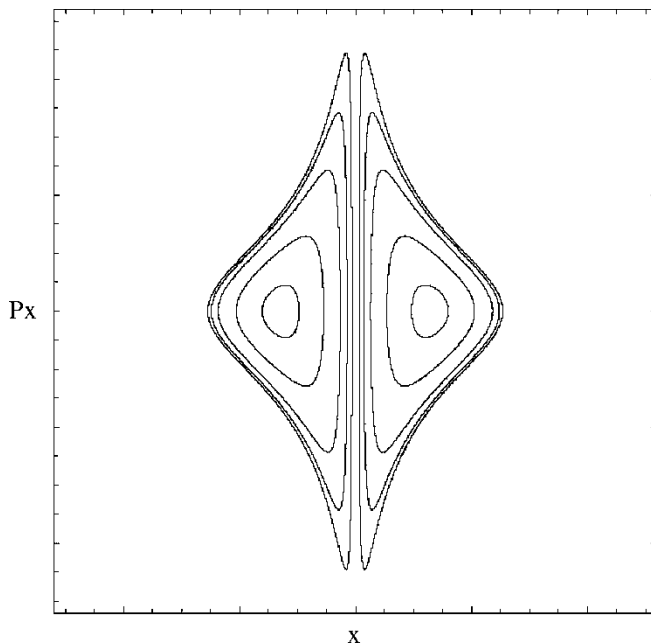


Figure 7. Theoretical $x - p_x$ phase plane. The values of parameters are as in figure 1.

4. Discussion

In this paper we have made an effort to describe and study the dynamical behaviour of a simple model of a Seyfert 1 galaxy. The model consists of a “bare” Seyfert 1 nucleus. We have chosen to study this case because recent observations indicate the existence of this kind of active galaxy. In particular, we were interested in the situation in which the model galaxy was subject to external perturbation caused by nearby galaxies.

Numerical calculations show that, for small external perturbations, the motion is regular with small chaotic regions. For large external perturbations the chaotic regions are very large. Here we must emphasize that the chaotic behaviour is a consequence of the external perturbation and does not come from the nuclear activity as in other cases [12, 14]. This comes from the fact that, when the external perturbation is absent, the model is axially symmetric. Furthermore, note that the nearby companions cause small chaotic regions, even for very small perturbations (see figure 1).

The role of the angular momentum is very important in this case as it was in the previous studied cases [15]. Orbits with small values of $\langle L \rangle$ are chaotic while orbits with large values of $\langle L \rangle$ are regular. Here we must make clear that, for about two decades since early work [18], we always find that the angular momentum is a very critical parameter, which is strongly connected to chaos in galactic models (see also [11]).

Another interesting result is that of the escaping orbits. When the ZNC is open there are orbits that escape to infinity. It was found that the majority of orbits escape in relatively small time periods but there are also some orbits, that remain for large time periods inside the open ZVC before escaping. In most cases those time periods are comparable to the age of the universe. In addition to the escaping orbits there are orbits that do not escape at all. These trapped orbits produce invariants curves around the stable direct end retrograde invariant points.

Finally we must not forget that the general characteristics of the system are qualitatively explained, for small external perturbations, using a quasi-integral of motion which can be considered as a generalization of the star's angular momentum.

References

- [1] S. Shapiro and S. Teukolsky, *Astrophys. J.* **292** L41 (1985).
- [2] Hernquist, *Nature* **340** 687 (1989).
- [3] E. Smith and T. Heckman, *Astrophys. J.* **348** 38 (1990).
- [4] H.R. Schmitt, J.L. Donley, R.R.J. Antonucci, J.B. Hutchings and A.L. Kinney, *Astrophys. J. Suppl.* **148** 327 (2003a).
- [5] H.R. Schmitt, J.L. Donley, R.R.J. Antonucci, J.B. Hutchings, A.L. Kinney and J.E. Pringle, *Astrophys. J.* **597** 768 (2003b).
- [6] S. Veilleux, P.L. Shopbell and S.T. Miller, *Astron. J.* **121** 198 (2001).
- [7] V. Das, D.M. Crenshaw and S.B. Kraemer, *Astron. J.* **656** 699 (2007).
- [8] V. Das, D.M. Crenshaw, S.B. Kraemer and R.P. Deo, *Astron. J.* **132** 620 (2006).
- [9] V. Das *et al.*, *Astron. J.* **130** 945 (2005).
- [10] J.E. Everett and N. Murray, *Astrophys. J.* **656** 93 (2007).
- [11] N.D. Caranicolas and N.J. Papadopoulos, *Astron. Astrophys.* **399** 957 (2003).
- [12] N.J. Papadopoulos and N.D. Caranicolas, *New Astron.* **1212** 11 (2006).
- [13] Vaughan *et al.*, *Monthly Notices of the Royal Astron. Soc.* **351** 193 (2004).
- [14] N.J. Papadopoulos and N.D. Caranicolas, *Astron. Nachrichten* **326**(2) 96 (2005).
- [15] N.D. Caranicolas and N.J. Papadopoulos, *Baltic Astron.* **14** 535 (2005).
- [16] N.D. Caranicolas, *New Astron.* **5** 397 (2000).
- [17] J. Binney and S. Tremaine, *Galactic Astronomy*, Princeton University Press, Princeton, NJ (1987).
- [18] N.D. Caranicolas and K.A. Innanen, *Astron. J.* **102** 1343 (1991).